AN EFFICIENT HERMITE REPRODUCING KERNEL MESHFREE METHOD FOR BUCKLING ANALYSIS OF KIRCHHOFF PLATES

Dongdong Wang[a)] & Huikai Peng
Department of Civil Engineering, Xiamen University, Xiamen, Fujian 361005, China

Summary A Hermite reproducing kernel Galerkin meshfree approach is presented for buckling analysis of Kirchhoff plates. In the Hermite reproducing kernel meshfree approximation the plate deflection is approximated by the deflection as well as rotation nodal variables. The resulting HRK shape function turns out to have a smaller minimum support size than its standard reproducing kernel counterpart from the solvability of the reproducing kernel moment matrix. The numerical integration of the material and geometric stiffness matrices is carried out in a unified manner by the sub-domain stabilized conforming integration method. A series of benchmark plate buckling examples show that the proposed method is very robust and accurate.

INTRODUCTION

Buckling analysis of Kirchhoff plates is of great importance for engineering deign. The C^1 continuity requirement for both the trial and test functions associated with the variational formulation of Kirchhoff plates poses severe difficulty for the conventional finite element method since the construction of C^1 conforming finite element approximation is not trivial. While on the other hand in the category of meshfree methods [1-3] which have gained significant research attention during the past two decades, the approximation of field variable can be customized with arbitrary high order global smoothness in a very straightforward way. In this study a new Hermite reproducing kernel (HRK) approximation and a sub-domain stabilized conforming integration (SSCI) method [2, 3] are presented for Kirchhoff plate buckling analysis. It is shown that the HRK approximation has better kernel stability with a smaller minimum normalized support size compared with that of the standard RK approximation. The numerical integration of the material and geometric stiffness matrices is carried out in a unified manner by the sub-domain stabilized conforming integration (SSCI) method. The SSCI method relies on the strain smoothing operation within each integration sub-domain. For the integration of the material stiffness matrix, SSCI involves the first order derivative of the shape function, while only the shape function itself is needed in SSCI for the geometric stiffness integration. A series of benchmark examples are employed to verify the effectiveness of the present method.

ALGORITHM FORMULATION

HRK meshfree approximation

In HRK approximation, the mid-plane domain Ω is discretized by a set of meshfree particles $\mathbf{x}_I$, $I = 1, 2, \cdots\cdots, NP$, the HRK approximation of the deflection $w(\boldsymbol{x})$, denoted by $w^h(\boldsymbol{x})$, can be expressed as:

$$w^h(\mathbf{x}) = \sum_{I=1}^{NP}\left[\Psi_I^w(\mathbf{x})w_I + \Psi_I^{\theta x}(\mathbf{x})\theta_{xI} + \Psi_I^{\theta y}(\mathbf{x})\theta_{yI}\right] = \sum_{I=1}^{NP}\mathbf{\Psi}_I(\mathbf{x})\mathbf{d}_I,\quad \mathbf{d}_I = \{w_I, \theta_{xI}, \theta_{yI}\}^T \tag{1}$$

where $\mathbf{\Psi}_I(\boldsymbol{x})=\{\Psi_I^w(\boldsymbol{x}), \Psi_I^{\theta x}(\boldsymbol{x}), \Psi_I^{\theta y}(\boldsymbol{x})\}$, $\Psi_I^w(\boldsymbol{x})$, $\Psi_I^{\theta x}(\boldsymbol{x})$ and $\Psi_I^{\theta y}(\boldsymbol{x})$ are the deflectional and rotational shape functions of node I, which take the following form:

$$\Psi_I^w(\boldsymbol{x}) = \mathbf{p}^T(\boldsymbol{x}_I - \boldsymbol{x})\mathbf{b}(\mathbf{x})\phi_a(\boldsymbol{x}_I - \boldsymbol{x}),\ \Psi_I^{\theta x}(\boldsymbol{x}) = \mathbf{p}_x^T(\boldsymbol{x}_I - \boldsymbol{x})\mathbf{b}(\mathbf{x})\phi_a(\boldsymbol{x}_I - \boldsymbol{x}),\ \Psi_I^{\theta y}(\boldsymbol{x}) = \mathbf{p}_y^T(\boldsymbol{x}_I - \boldsymbol{x})\mathbf{b}(\mathbf{x})\phi_a(\boldsymbol{x}_I - \boldsymbol{x}) \tag{2}$$

where $\mathbf{b}(\mathbf{x})$ is the unknown position dependent coefficient vector to be solved. $\phi_a(\boldsymbol{x}_I - \boldsymbol{x})$ is the kernel function centering at node I which has a compact support measured by 'a'. In this work the cubic B-spline kernel function is employed. The n-th order monomial basis vectors $\mathbf{p}$, $\mathbf{p}_x$, and $\mathbf{p}_y$ are defined as:

$$\mathbf{p}(\mathbf{x}) = \left\{1,\ x,\ y,\ x^2,\ xy,\ y^2, ..., x^n,\ ...,\ y^n\right\}^T,\ \mathbf{p}_x(\mathbf{x}) = \partial\mathbf{p}(\mathbf{x})/\partial x,\ \mathbf{p}_y(\mathbf{x}) = \partial\mathbf{p}(\mathbf{x})/\partial y \tag{3}$$

Gradient smoothing and SSCI Discrete equations

The key idea for the SSCI method is the strain smoothing [1-3]. In SSCI Ω_L is sub-divided into LS non-overlapping and conforming sub-domains. The voronoi diagram can be used to construct the nodal representative domain Ω_L as indicated in Fig. 1(a). Thereafter the sub-domain can be further obtained by subdividing the nodal representative domain through connecting the node and the edge middle points of voronoi diagram. It is noted the only

[a)] Corresponding author. Email: ddwang@xmu.edu.cn.

requirement for the sub-domains is to construct conforming cells for domain integration and thus other choices for sub-domains are also possible. The smoothed rotation $\tilde{\boldsymbol{\theta}}^h$ and curvature $\tilde{\boldsymbol{\kappa}}$ in Ω_{L_m} are defined as:

$$\tilde{\boldsymbol{\kappa}}^h(\mathbf{x}_{L_m}) = \sum_{I=1}^{NP} \tilde{\mathbf{B}}_I^k(\mathbf{x}_{L_m})\mathbf{d}_I,\ \tilde{\mathbf{B}}_I^k = \begin{bmatrix} \tilde{\nabla}_x \Psi_{I,x}^w & \tilde{\nabla}_x \Psi_{I,x}^{\theta x} & \tilde{\nabla}_x \Psi_{I,x}^{\theta y} \\ \tilde{\nabla}_x \Psi_{I,y}^w & \tilde{\nabla}_x \Psi_{I,y}^{\theta x} & \tilde{\nabla}_x \Psi_{I,y}^{\theta y} \\ 2\tilde{\nabla}_y \Psi_{I,x}^w & 2\tilde{\nabla}_y \Psi_{I,x}^{\theta x} & 2\tilde{\nabla}_y \Psi_{I,x}^{\theta y} \end{bmatrix}, \tilde{\nabla}_j \boldsymbol{\Psi}_{I,i}(\mathbf{x}_{L_m}) = (A_{L_m})^{-1}\int_{\Gamma_{L_m}} [\Psi_{I,i}^w, \Psi_{I,i}^{\theta x}, \Psi_{I,i}^{\theta y}] n_j \, d\Gamma \quad (4)$$

$$\tilde{\boldsymbol{\theta}}^h(\mathbf{x}_{L_m}) = \sum_{I=1}^{NP} \tilde{\mathbf{B}}_I^g(\mathbf{x}_{L_m})\mathbf{d}_I,\ \tilde{\mathbf{B}}_I^g = \begin{bmatrix} \tilde{\nabla}_x \Psi_I^w & \tilde{\nabla}_x \Psi_I^{\theta x} & \tilde{\nabla}_x \Psi_I^{\theta y} \\ \tilde{\nabla}_y \Psi_I^w & \tilde{\nabla}_y \Psi_I^{\theta x} & \tilde{\nabla}_y \Psi_I^{\theta y} \end{bmatrix}, \ \tilde{\nabla}_i \boldsymbol{\Psi}_I(\mathbf{x}_{L_m}) = (A_{L_m})^{-1}\int_{\Gamma_{L_m}} [\Psi_I^w, \Psi_I^{\theta x}, \Psi_I^{\theta y}] n_i \, d\Gamma \quad (5)$$

where the details of the geometric notations can be found from Fig. 1(a). The resulting discrete meshfree equations for buckling analysis are:

$$\mathbf{Kd} = \lambda \mathbf{K}^g \mathbf{d},\ \mathbf{K}_{IJ} = \sum_{K=1}^{NP} \sum_{K_i=1}^{IK} \tilde{\mathbf{B}}_I^{k^T}(\mathbf{x}_{K_i})\mathbf{D}\tilde{\mathbf{B}}_J^k(\mathbf{x}_{K_i})A_{K_i},\ \mathbf{K}_{IJ}^g = \sum_{K=1}^{NP} \sum_{K_i=1}^{IK} \tilde{\mathbf{B}}_I^{g^T}(\mathbf{x}_{K_i})\boldsymbol{\sigma}\tilde{\mathbf{B}}_J^g(\mathbf{x}_{K_i})A_{K_i} \quad (6)$$

with $\mathbf{D}$ and $\boldsymbol{\sigma}$ being the plate constitutive matrix and initial stress matrix, λ being the buckling load to be solved..

RESULTS AND CONCLUSIONS

Consider a simply supported circular plate as shown in Fig. 1(b). The material and geometry parameters are: Young's modulus $E = 2\times 10^{11}$, Poisson ratio $\upsilon = 0.3$, plate radius $r = 5$, and thickness $t = 0.05$. The HRK approximation with quadratic basis function and cubic B-spline kernel function with normalized support size of 1.3 are used. The convergence behavior of the fundamental frequency is shown in Fig. 1(c) and the first five buckling modes are listed in Fig. 1(d). The results of Fig. 1(c) clearly also show that the present SSCI approach performs superiorly compared to the meshfree formulations with 2-point (GI2) and 6-point Gauss integrations for stiffness evaluation.

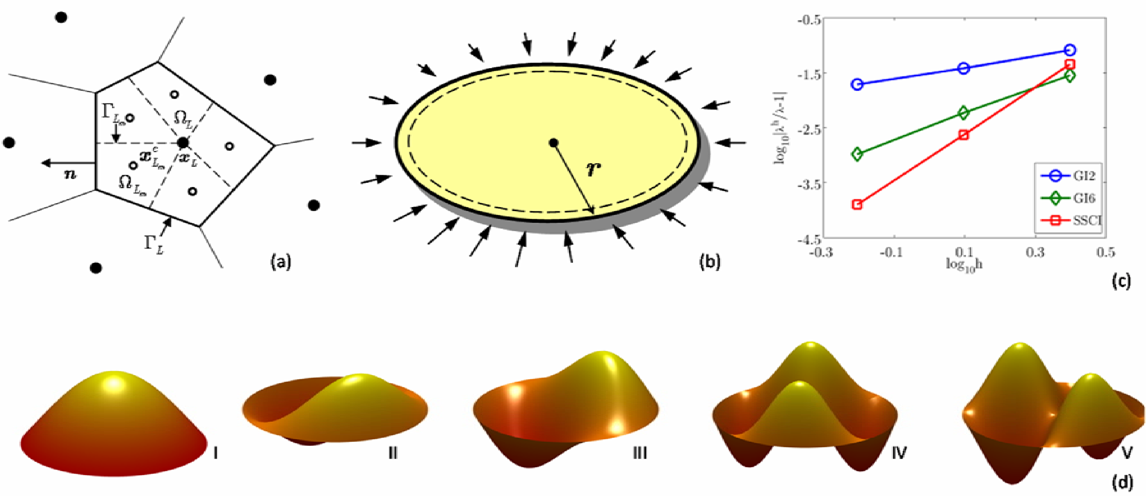

Figure 1: (a) Nodal representative domain; (b) Simply supported circular plate; (c) Comparison of convergence rate of the critical buckling load of the circular plate; (d) First five buckling modes of the circular plate

ACKNOWLEDGEMENTS

The financial support of this work by the National Natural Science Foundation of China (10972188), the Program for New Century Excellent Talents in University from China Education Ministry (NCET-09-0678), and the Fundamental Research Funds for the Central Universities of China (2010121073) is gratefully acknowledged.

References

[1] Chen J.S., Wu C.T., Yoon S., You Y.: A stabilized conforming nodal integration for Galerkin meshfree methods. *International Journal for Numerical Methods in Engineering* **50**:435-466, 2001.

[2] Wang D., Chen J. S.: A Hermite reproducing kernel approximation for thin plate analysis with sub-domain stabilized conforming integration, *International Journal for Numerical Methods in Engineering* **74**: 368-390, 2008.

[3] Wang D., Lin Z.: Dispersion and transient analyses of Hermite reproducing kernel Galerkin meshfree method with sub-domain stabilized conforming integration for thin beam and plate structures, Computational Mechanics, **48**: 47-63, 2011.